Crystal Structure of Tryptophan Hydroxylase with Bound Amino Acid Substrate[†,‡]

Michael S. Windahl,[§,||] Charlotte R. Petersen,[||,⊥] Hans E. M. Christensen,*[,||] and Pernille Harris*[,||]

Department of Basic Sciences and Environment, Faculty of Life Sciences, University of Copenhagen, Thorvaldsensvej 40, 1871 Frederiksberg C, Denmark, and Department of Chemistry, Building 207, Technical University of Denmark, 2800 Kgs. Lyngby, Denmark

Received August 13, 2008; Revised Manuscript Received September 8, 2008

ABSTRACT: Tryptophan hydroxylase (TPH) is a mononuclear non-heme iron enzyme, which catalyzes the reaction between tryptophan, O_2, and tetrahydrobiopterin (BH_4) to produce 5-hydroxytryptophan and 4a-hydroxytetrahydrobiopterin. This is the first and rate-limiting step in the biosynthesis of the neurotransmitter and hormone serotonin (5-hydroxytryptamine). We have determined the 1.9 Å resolution crystal structure of the catalytic domain (Δ1−100/Δ415−445) of chicken TPH isoform 1 (TPH1) in complex with the tryptophan substrate and an iron-bound imidazole. This is the first structure of any aromatic amino acid hydroxylase with bound natural amino acid substrate. The iron coordination can be described as distorted trigonal bipyramidal coordination with His273, His278, and Glu318 (partially bidentate) and one imidazole as ligands. The tryptophan stacks against Pro269 with a distance of 3.9 Å between the iron and the tryptophan Cζ3 atom that is hydroxylated. The binding of tryptophan and maybe the imidazole has caused the structural changes in the catalytic domain compared to the structure of the human TPH1 without tryptophan. The structure of chicken TPH1 is more compact, and the loops of residues Leu124−Asp139 and Ile367−Thr369 close around the active site. Similar structural changes are seen in the catalytic domain of phenylalanine hydroxylase (PAH) upon binding of substrate analogues norleucine and thienylalanine to the PAH·BH_4 complex. In fact, the chicken TPH1·Trp·imidazole structure resembles the PAH·BH_4·thienylalanine structure more (root-mean-square deviation for Cα atoms of 0.90 Å) than the human TPH1 structure (root-mean-square deviation of 1.47 Å).

Tryptophan hydroxylase (TPH,[1] EC 1.14.16.4) catalyzes the hydroxylation of tryptophan to 5-hydroxytryptophan, which is the first and rate-limiting step in the biosynthesis of serotonin (*1*). Serotonin is an important neurotransmitter, and dysfunction of the central serotonergic system is observed in psychiatric disorders such as depression, obsessive-compulsive disorder, and schizophrenia (*2*). Tryptophan hydroxylase exists in two isoforms (*3*). Isoform 2 (TPH2) is responsible for tryptophan hydroxylation in the brain (*4*), while isoform 1 (TPH1) mainly is expressed in the peripheral parts of the body (*5*) and in the pineal gland (*6*). In the pineal gland, 5-hydroxytryptophan also serves as a precursor in biosynthesis of the hormone melatonin which is involved in daily rhythm control (*7*).

TPH is part of the enzyme family of tetrahydrobiopterin-dependent aromatic amino acid hydroxylases. In addition to TPH, this family includes phenylalanine hydroxylase (PAH, EC 1.14.16.1) and tyrosine hydroxylase (TH, EC 1.14.16.2) (*8*). All three enzymes use tetrahydrobiopterin and O_2 to hydroxylate the respective aromatic amino acids and are believed to follow the same reaction mechanism (*9, 10*). The aromatic amino acid hydroxylases are mononuclear iron oxygenases with the iron coordinated by the two histidines and one glutamate, and this 2-histidine-1-carboxylate facial triad iron coordination is a well-known motif in many mononuclear non-heme iron(II) enzymes (*11*). The eukaryotic aromatic amino acid hydroxylases all form homotetramers, and each monomer can be divided into an N-terminal regulatory domain, a catalytic domain, and a small tetramerization domain in the C-terminus (*8*).

Different truncation variants of all three aromatic amino acid hydroxylases have been structurally characterized. In the case of PAH, structures of the catalytic domain with iron in the ferrous (PDB entries 1J8T and 1J8U) and ferric state (PDB entry 1PAH) are available (*12, 13*), with and without the cosubstrate 5,6,7,8-tetrahydro-L-biopterin (BH_4) (PDB entries 1J8U and 1J8T, respectively) (*12*). No overall structural differences are seen when the ferric and ferrous structures of the catalytic domain are compared (*12*). The

† This study was supported by grants to H.E.M.C. from The Novo Nordisk Foundation (1689) and The Danish Medical Research Council (271-05-0318). The Graduate School on Metal Ions in Biological Systems and Technical University of Denmark provided a Ph.D. scholarship for M.S.W.

‡ The coordinates have been deposited in the Protein Data Bank as entry 3E2T.

* To whom correspondence should be addressed. H.E.M.C.: telephone, +45 45 25 23 47; fax, +45 45 88 31 36; e-mail, hemc@kemi.dtu.dk. P.H.: telephone, +45 45 25 20 24; fax, +45 45 88 31 36; e-mail, ph@kemi.dtu.dk.

§ University of Copenhagen.

|| Technical University of Denmark.

⊥ Present address: Department of Medicinal Chemistry, Faculty of Pharmaceutical Sciences, University of Copenhagen, Copenhagen, Denmark.

[1] Abbreviations: TPH, tryptophan hydroxylase; TPH2, tryptophan hydroxylase isoform 2; TPH1, tryptophan hydroxylase isoform 1; PAH, phenylalanine hydroxylase; TH, tyrosine hydroxylase; BH_4, (6*R*)-5,6,7,8-tetrahydro-L-biopterin; THA, 3-(2-thienyl)-L-alanine; NLE, L-norleucine; cTPH1, catalytic domain of tryptophan hydroxylase isoform 1; BH_2, (6*R*)-7,8-dihydro-L-biopterin; rmsd, root-mean-square deviation; Im, imidazole; PDB, Protein Data Bank.

10.1021/bi8015263 CCC: $40.75
Published on Web 10/21/2008

binding of BH_4 causes small structural changes in the BH_4 binding pocket, but again no large overall change in the structure is observed (*12*). It has not been possible to obtain structures with both BH_4 and the natural amino acid, but instead, structures of the ternary complexes with BH_4 and the substrate analogues 3-(2-thienyl)-L-alanine (THA) (PDB entries 1KW0 and 1MMK) and L-norleucine (NLE) (PDB entry 1MMT) are available (*14, 15*). Comparison of the structures PAH-Fe(II)·BH_4·THA and PAH-Fe(II)·BH_4·NLE to the PAH-Fe(II)·BH_4 structure reveals large structural changes (*14, 15*). The structural changes are seen throughout the catalytic domain but most notably in the loop region containing residues 133−141, where Tyr138 of this loop moves from a surface position in the PAH-Fe(II)·BH_4 structure (PDB entry 1J8U) to a partially buried position close to the active site in the PAH-Fe(II)·BH_4·THA structure (PDB entry 1MMK) (*15*).

The corresponding loop in TH has recently been studied via a mutational study and fluorescence anisotropy (*16, 17*). These studies showed that the loop (residues 178−193 in TH) is similarly mobile (*17*) and that the side chains of the residues in the loop, especially Phe184 (corresponding to Tyr138 in PAH), are important in the formation of the proper amino acid substrate binding site (*16*). The fluorescence anisotropy study showed that the binding of BH_4 to TH rather than the amino acid substrate binding caused the conformational change in the loop (*17*).

TPH has not been structurally characterized to the extent of PAH and TH, and the only crystal structure of TPH is of the catalytic (c) domain of human TPH1 (cTPH1) with bound 7,8-dihydrobiopterin (BH_2) and ferric iron (PDB entry 1MLW) (*18*). This structure is similar to the structures of the catalytic domain of PAH with either BH_4 or BH_2 bound (*12, 19*). In the human cTPH1 structure, Tyr125 (corresponding to Tyr138 in PAH) is positioned in a surface position, and the loop region corresponding to the flexible loop in TH and PAH is refined with high *B*-factors, indicating that this loop might be dynamic in a manner similar to that of TH and PAH. Studies of structural changes in TPH upon tryptophan and/or BH_4 binding have not previously been performed.

We have previously reported the expression, purification, and crystallization of chicken (*Gallus gallus*) cTPH1 (Δ1−100/Δ415−445) (*20*). We here present the crystal structure of the ferric form of chicken cTPH1 with bound tryptophan in the active site. This is the first structure of any aromatic amino acid hydroxylase with its natural amino acid substrate bound.

MATERIALS AND METHODS

Ultrapure glycerol was obtained from Invitrogen. The solution of 0.2 M imidazole malate (pH 8.5) and 22.5% PEG 10000 was from Molecular Dimensions. All chemicals used were analytical grade obtained from Sigma-Aldrich. All solutions were prepared using 18.2 MΩ cm water from a Milli-Q synthesis A10 Q-Gard system (Millipore). Chicken (*G. gallus*) cTPH1 (Δ1−100/Δ415−445)[2] was expressed and purified as described previously (*20*).

[2] Chicken TPH1 contains one more residue in the regulatory domain compared to human TPH1.

Table 1: Data and Refinement Statistics

beamline	ESRF, ID 14-3
detector	ADSC, Quantum 4
temperature (K)	100
wavelength (Å)	0.934
resolution range (Å)	48.4−1.90 (2.0−1.90)[a]
no. of reflections	214775 (30024)[a]
no. of unique reflections	30024 (4233)[a]
redundancy	7.2 (7.2)[a]
completeness (%)	100 (100)[a]
R_{merge} (%)[b]	0.146 (0.547)[a]
$\langle I/\sigma(I)\rangle$	13.84 (2.61)[a]
crystal space group	$C222_1$
unit cell parameters	
a (Å)	78.0
b (Å)	155.3
c (Å)	61.8
Mathews coefficient, V_M (Å^3/Da)	2.38
refinement	
no. of reflections in working set	28520
no. of reflections in test set	1502
R_{work}/R_{free} (%)[c]	18.2/22.6
diffraction-component precision index (Cruickshanks) (Å)	0.14
rmsd from ideal geometry	
bond lengths (Å)	0.012
bond angles (deg)	1.275
total no. of atoms in the asymmetric unit	2804
protein	2546
iron	1
imidazole	5
L-tryptophan	15
triethylene glycol	20
sulfate, 50% occupancy	5
water	219
average *B*-factor (Å^2)	
main chain	15.7
side chain	17.5
iron	6.8
tryptophan	9.9
imidazole	16.6
water	23.3

[a] Values in parenthesis are for the outermost resolution shell. [b] $R_{merge} = \sum_i|I_i - \langle I_i\rangle|/\sum_i I_i$, where $\langle I_i\rangle$ is the average of I_i over all symmetry equivalents. [c] $R = \sum_{work} ||F_{obs}| - k|F_{calc}||/\sum_{work} |F_{obs}|$ and $R_{free} = \sum_{test} ||F_{obs}| - k|F_{calc}||/\sum_{test} |F_{obs}|$, where $|F_{obs}|$ and $|F_{calc}|$ are observed and calculated structure factor amplitudes for all reflections (*R*-factor) and the reflections applied in the test R_{free} set, respectively.

Crystallization and Data Collection. The initial crystallization trials have been described previously (*20*). Crystallization of chicken cTPH1 was conducted using the vapor diffusion method with sitting drops (2 + 2 μL in size). The reservoir solution contained 0.2 M imidazole malate (pH 8.5) and 22.5% PEG 10000. The chicken cTPH1 concentration in the protein solution was 2.8 mg/mL as determined by an ε_{280} of 37820 M^{-1} cm^{-1} (HP 8453 diode array spectrophotometer). The tray was placed on ice during drop setup and was subsequently stored at 4 °C. Crystals appeared after 6 months. The crystals were flash-cooled with the mother liquor and subsequently annealed by being transferred to 20% PEG 400, 0.2 M imidazole malate (pH 8.5), and 22.5% PEG 10000, and immediately the crystals were again flash-cooled. Data were collected on beamline ID 14-3 at the European Synchrotron Radiation Facility. The data were processed in space group $C222_1$ using XDS and X-scale (*21*) (see Table 1 for data statistics). The structure was determined by molecular replacement using the structure of the catalytic domain of human PAH (PDB entry 1PAH) (*13*) as a search model. This structure was chosen because it was crystallized

with only iron bound as we believed was the case for our chicken cTPH1 crystals. The level of sequence identity of the catalytic domains of human PAH and chicken TPH1 is 63%.

Refinement. Refinement was carried out using REFMAC5 (*22*) in the CPP4 suite (*23*), and visual inspections and model rebuilding were carried out using WinCoot (*24*). The initial electron density was poor in large areas, but by rebuilding large parts of protein chain, we were able to obtain well-defined electron density for residues 105−411. The final model contains residues 105−411, one iron, one tryptophan molecule, one imidazole molecule, one sulfate ion (50% occupancy), two triethylene glycol molecules, and 219 water molecules. The following residues were refined with alternate conformations: Leu124, Ser261, Leu281, Ser349, Arg388, Val400, Ser408, and Val409. The model was refined to an *R*-factor of 0.182 and an R_{free} of 0.226. The refinement statistics are listed in Table 1.

The structure was validated using PROCHECK (*25*), and the Ramachandran plot shows 90% of the residues in the most favored region and 10% of the residues in the additionally allowed regions. Structure-based alignment was conducted using TOP (*26*). Graphics illustrating the protein structure were made using Pymol (*27*). Structural analysis for hinge regions was conducted using DynDom (*28*).

RESULTS AND DISCUSSION

The crystal structure of chicken cTPH1 containing 307 residues (105−411), one iron, one L-tryptophan molecule, and one imidazole molecule was determined to 1.9 Å resolution. This is the first crystal structure of any aromatic amino acid hydroxylase with its natural amino acid substrate bound in the active site. The chicken cTPH1 used for crystallization contains residues 101−414, but there was no visible electron density for residues 101−104 or 412−414. The overall structure of chicken cTPH1 is similar to that of the catalytic domain of the other aromatic amino acid hydroxylases, i.e., PAH and TH (*13, 29*). The chicken cTPH1 structure resembles the structure of PAH with bound THA and BH_4 (PDB entry 1MMK) (*15*) more than the structure of human cTPH1 (PDB entry 1MLW) with root-mean-square deviations for the Cα atoms of 0.90 and 1.47 Å, respectively. The structural alignment of the chicken cTPH1 structure with the human cTPH1 structure is shown in Figure 1.

Crystallization Time. The crystallization time for the chicken cTPH1 crystals was 3−6 months. When the chicken cTPH1 drops were set up, strong precipitation was always observed. While the imidazole bound in the active site originated from the crystallization solution, the tryptophan also bound in the active site was not added to the purification or crystallization solutions. Most likely, tryptophan has been bound in the active site of chicken cTPH1 from the time of expression in the *Escherichia coli* cells. The tryptophan could also have been formed from proteolytic degradation of chicken cTPH1 molecules. This could explain the very long crystallization time, but since only two tryptophans are present in chicken cTPH1, both are visible in the structure, and none of these are found in the termini, this is not the likely source of the tryptophan.

Tryptophan Binding. The electron density for the substrate tryptophan is well-defined, and the average *B*-factor of the

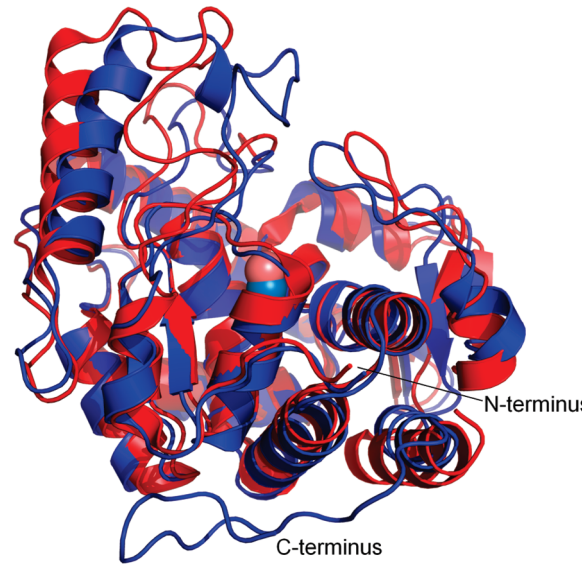

FIGURE 1: Structural alignment of chicken cTPH1 (blue) and human cTPH1 (red, PDB entry 1MLW) (*18*) with the irons shown as spheres. Large structural differences are seen throughout the structure, most clearly in the loops above the active site. The expression construct of chicken cTPH1 is elongated in the C-terminus compared to the human cTPH1 construct that was used (*18*), and this C-terminal part is visible in the chicken cTPH1 structure.

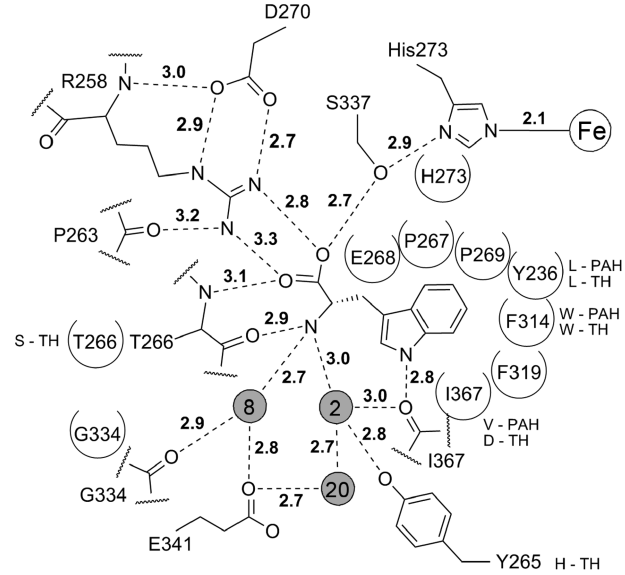

FIGURE 2: Schematic view of the tryptophan substrate interactions in chicken cTPH1. Hydrogen bonds are shown as dashed lines, and the filled gray circles represent water molecules. Semicircled residues have hydrophobic interactions with the tryptophan. For residues which are not conserved in PAH and TH, the corresponding residue is shown.

tryptophan is 9.9 Å^2. The interactions between the tryptophan and chicken cTPH1 are shown in Figure 2. The hydrophobic part of the tryptophan binding pocket is lined with the side chains of Tyr236, Thr266, Pro269 (ring stacking), His273, Phe314, Phe319, and Ile367 and with the backbone of Pro267, Glu268, and Gly334. The polar interactions of the tryptophan are between Thr266 N and Trp O1 (3.1 Å), Thr266 O and Trp N (2.9 Å), and Ile367 O and Trp Nε1 (2.8 Å) and with side chains Arg258 Nη1 and Trp O1 (3.3 Å), Arg258 Nη2 and Trp O2 (2.8 Å), and Ser337 Oγ and Trp O2 (2.6 Å). Additionally, water molecules water2 and

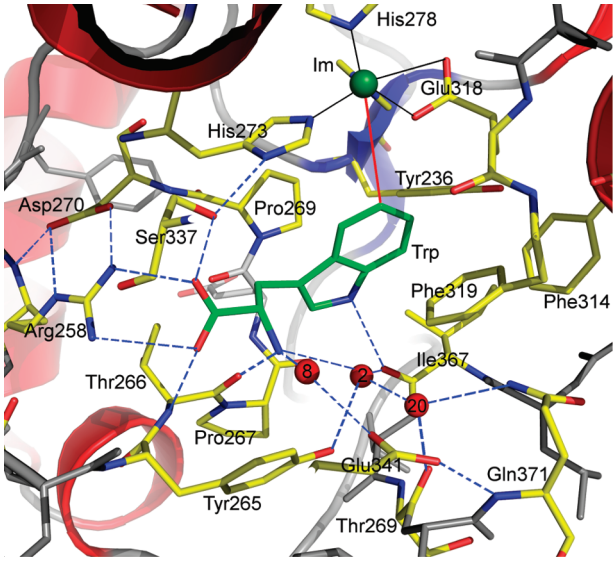

FIGURE 3: Tryptophan binding in the active site. The hydrogen bonds and covalent bonds of the iron are shown with dashed blue lines and black lines, respectively. The distance from tryptophan Cζ3 to the iron (red line) is 3.9 Å. Water molecules are shown as red spheres. Imidazole is abbreviated Im.

water8 are hydrogen bonded to Trp N (3.0 and 2.7 Å, respectively). Water2 also hydrogen bonds to Ile367 O (3.0 Å), Tyr265 Oη (2.8 Å), and water20 (2.7 Å), and water8 also hydrogen bonds to Glu341 Oε1 (2.8 Å) and Gly334 O (2.9 Å). The distance between tryptophan Cζ3 that is hydroxylated and the iron is 3.9 Å (see Figure 3). The angle between the tryptophan plane and iron is 141° (measured Fe−Cζ3−Cε2 angle). The structure of the catalytic domain of PAH with the substrate analogue THA has been determined (PDB entry 1MMK) (*15*). The binding of THA in PAH is similar to that of tryptophan in chicken cTPH1 with regard to the polar interactions, but the ring system of THA stacks onto the imidazole group of His285 (*14*) while the tryptophan is positioned sideways with respect to the corresponding His273 (see Figure 4). Instead, tryptophan stacks on Pro269, yielding an angle between the tryptophan plane and the iron of 141° rather than the angle of 101° between the THA ring and the iron (Fe−Cε2−Cβ) (*15*).

Substrate Specificity. The substrate specificity in the aromatic amino acid hydroxylases must be controlled through the interactions of the side chain of the amino acid substrate. The side chain of the tryptophan substrate is bound in a hydrophobic pocket lined by residues Tyr236, Thr266, Pro267, Glu268, Pro269, His273, Phe314, Phe319, and Ile367 (see Figures 2 and 3). Of these, Tyr236, Phe314, and Ile367 are not conserved in PAH and TH and Thr266 is not conserved in TH.

The role of Tyr236 in substrate binding has previously been studied (*30*). Variants Y236A and Y236L had decreased levels of substrate inhibition and an increased apparent $K_{m,tryptophan}$. In the human cTPH1·BH_2 structure, Tyr236 is furthermore involved in the BH_2 binding, where the BH_2 is sandwiched between Tyr236 and Phe242 (*18*). The structure here confirms that Tyr236 is also involved in tryptophan binding (see Figure 3).

Phe314 has previously been identified as having an important role in the substrate specificity of TPH (*31, 32*). With a change from Phe314 to a tryptophan, which is seen in PAH and TH, the preference for tryptophan over phenylalanine was weakened (*31, 32*). The Phe314 instead of a tryptophan results in a larger binding cavity for the tryptophan substrate which in part governs the substrate specificity.

The residues corresponding to Ile367 are a valine in PAH and Asp425 in TH. Asp425 in TH is known to be important for the substrate specificity of TH, possibly by hydrogen bonding to the hydroxyl group of the tyrosine substrate to place it in the proper position for hydroxylation (*33*). In TPH, Ile367 forms part of the hydrophobic binding pocket and a charged/polar residue, such as aspartate, at this position may significantly disturb tryptophan binding.

Imidazole Binding. Structural alignment of the iron sites of human cTPH1-Fe(III)·BH_2 and chicken cTPH1-Fe(III)·Trp shows that the imidazole binds between the sites where the water molecules are bound in the human cTPH1 structure, with the imidazole pointing in the same direction as the position of BH_2 in the human cTPH1 structure. In the PAH-Fe(II)·BH_4·THA structure, BH_4 is bound closer to the iron, and a structural alignment of the iron site with the chicken cTPH1 structure (see Figure 4) shows that the BH_4 is located quite close to the position of imidazole in the chicken cTPH1 structure. The imidazole does not interact directly with the protein chain but interacts through two bridging water molecules with Gly235 O, Leu237 N, His252 O, and Glu274 Oε1, as shown in Figure 5. The BH_2 in human cTPH1 interacts directly with Leu236 N, Leu236 O, and Gly234 O and through bridging water molecules with His251 O, Glu273 Oε1, and Glu273 Oε2. BH_2 in human cTPH1 furthermore interacts through bridging water molecules with Glu317 and the iron. Since some of the hydrogen bonds in human cTPH1·BH_2 are still preserved by the imidazole in the chicken cTPH1 structure, the imidazole might mimic the BH_4/BH_2 binding in the active site.

Conformational Changes upon Tryptophan Binding. The binding of tryptophan and imidazole causes the chicken cTPH1 to change conformation to a more closed and compact structure compared to the human cTPH1 structure (see Figure 1). This gives a unique opportunity to investigate changes in TPH1 upon substrate binding. In a comparison of the structure to that of human cTPH1·BH_2, four hinge regions were identified: residues 121−134, 148 and 149, 162 and 163, and 168 and 169. Comparison of the crystal structures of PAH revealed large movement in the loop region of residues 131−155 upon binding of THA or NLE to the PAH-Fe(II)·BH_4 complex (*12, 14, 15*). Similarly, the largest differences between the structure of human cTPH1-Fe(III)·BH_2 and chicken cTPH1-Fe(III)·Trp are seen in the loop region of Leu124−Asp139 which moves toward the loop of Ile367−Thr369. The structural alignment of human cTPH1-Fe(III)·BH_2 and chicken cTPH1-Fe(III)·Trp structures in Figure 6 illustrates this movement. The two loops close around the active site, reducing the distances between Leu130 Cα and Thr368 Cα from 17.3 Å in human cTPH1-Fe(III)·BH_2 to 7.1 Å in chicken cTPH1-Fe(III)·Trp.

Tyr126 corresponds to Tyr138 in PAH, and crystal structures of PAH have shown that this tyrosine changes from a surface position to a buried position close to the active site upon binding of the substrate analogue THA or NLE (*12, 14, 15*). Tyr126 of chicken cTPH1 corresponds to Phe184 in TH. The movement of this phenylalanine residue and the flexibility of the loop in TH have been studied, and

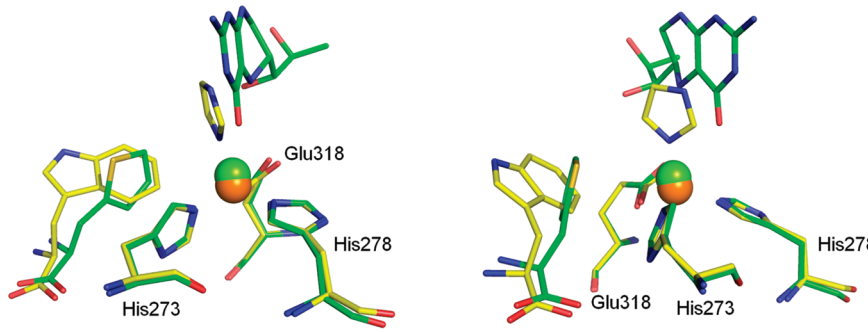

FIGURE 4: Two orientations of the structural alignment of the iron coordinating residues (His273, His278, and Glu319) of chicken cTPH1-Fe(III)·Trp (yellow) with the equivalent residues of PAH-Fe(II)·BH_4·THA (PDB entry 1MMK) (green). The THA packs against the closest iron coordinating histidine, while the substrate tryptophan is positioned sideways with respect to this histidine. The position of the imidazole is close to the position of BH_4 in the PAH-Fe(II)·BH_4·THA structure.

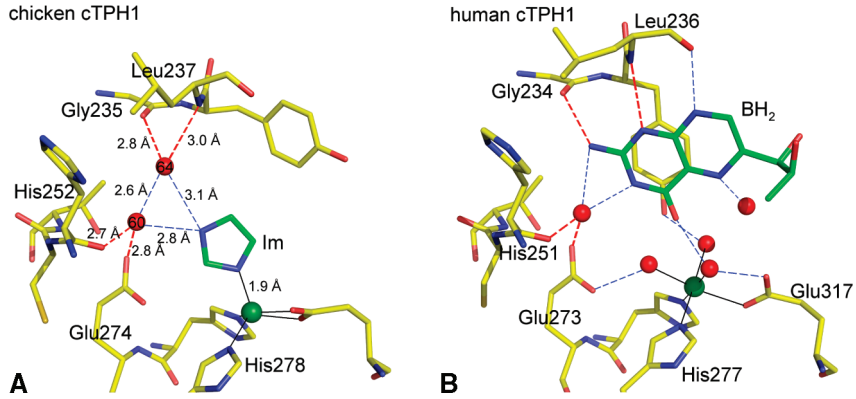

FIGURE 5: (A) Hydrogen bonds of the iron-coordinated imidazole. Water molecules are shown as red spheres, and the iron is shown as a green sphere. The imidazole forms bridging hydrogen bonds to Glu274 and His254 through water60 and to Gly235 and Leu237 through water64. (B) The hydrogen bonds formed by BH_2 in the human cTPH1 structure (PDB entry 1MLW) are similar. Direct hydrogen bonds are formed to Gly234 and to Leu236 N and O, while water-bridged hydrogen bonds formed to His251, Glu273, and Glu317 (*18*). The hydrogen bonds that are similar in both structures are colored red.

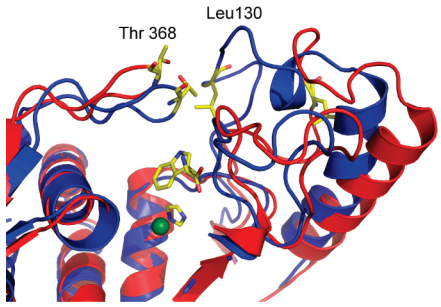

FIGURE 6: Aligned structures of chicken cTPH1·Trp (blue) and human cTPH1·BH_2 (red, PDB entry 1MLW) (*18*) showing the loops closing above the active site. Leu130 and Thr368 are shown with yellow sticks. The distance between the Cα atoms of Leu130 and Thr368 decreases from 17.3 Å in human cTPH1·BH_2 to 7.1 Å in chicken cTPH1·Trp.

a large movement is detected upon binding of BH_4 (*17*). The structural alignment of PAH-Fe(II)·BH_4·THA, human cTPH1-Fe(III)·BH_2, and chicken cTPH1-Fe(III)·Trp structures in Figure 7 shows that the loop of residues Asp117−Asp139 has quite different conformations. In chicken cTPH1, Tyr126 has not moved to a buried position, but the loop has made an extra turn, still keeping Tyr126 on the surface where it is packed against Phe137 and with a triethylene glycol molecule nearby (4 Å). Tyr126 cannot move to the position which is seen for the corresponding Tyr in PAH-Fe(II)·BH_4·THA (PDB entry 1MMK) (*15*) since it would then clash with Tyr236 and Ile367.

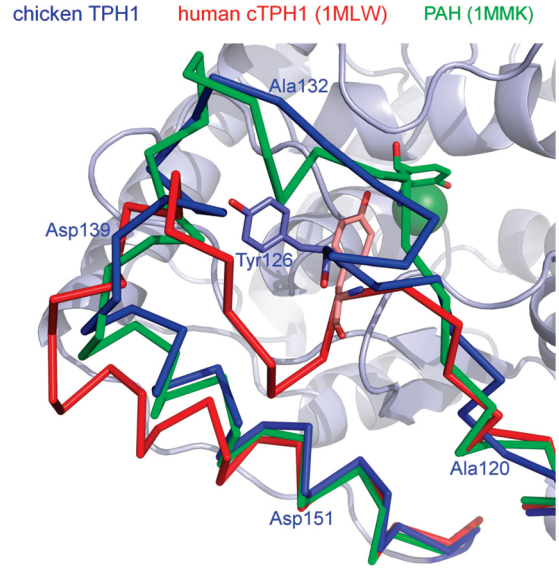

FIGURE 7: Structural alignment of flexible loop residues Asp117−Asp151 in chicken cTPH1 (blue) with human cTPH1 (red, PDB entry 1MLW) and PAH (green, PDB entry 1MMK). The chicken cTPH1 structure is colored light blue, and the iron is shown as a green sphere. Tyr126 is shown with sticks. Tyr126 is solvent-exposed in chicken cTPH1 while it is positioned in the interior of PAH close to the iron.

The kinetic mechanism of PAH and TH is a sequential mechanism, and the order of substrate binding is generally believed to be that BH_4 binds as the first substrate with the aromatic amino acid as the second or third (*34, 35*). None

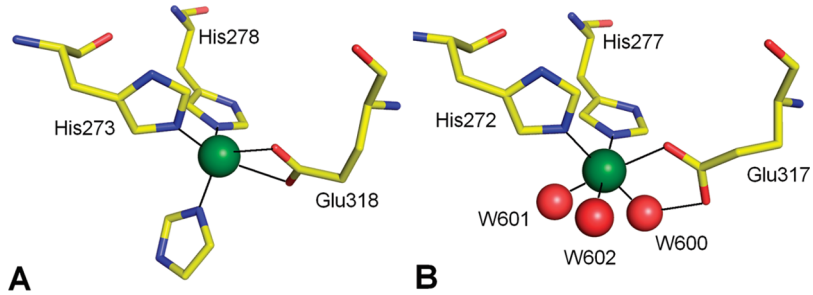

FIGURE 8: (A) Coordination of iron(III) (green sphere) by His273, His278, Glu318, and an imidazole. (B) Coordination of iron(III) in the human cTPH1·BH_2 structure by His272, His277, Glu317, and three water molecules (red spheres) (*18*).

of the structures of PAH, TH, and TPH contain the aromatic amino acid substrate, while several structures have BH_4 or the oxidized analogue BH_2 bound. This fact supports BH_4 as the first substrate to bind. The structures of PAH show that the binding of the BH_4 or BH_2 cosubstrate does not result in any major structural changes (*14*). We observe large structural changes upon binding of tryptophan without BH_4 or BH_2 bound, but with imidazole bound. This structure therefore raises the question of whether it is the aromatic amino acid binding or the combination of BH_4 and the aromatic amino acid that causes the conformational change.

Two different scenarios can be envisioned.

(1) The binding of tryptophan alone to TPH causes the structural changes observed in the present structure compared to the human cTPH1-Fe(III)·BH_2 structure. In this conformation, the tryptophan is trapped inside TPH, and this can explain how tryptophan is present in the structure even though it was not added during purification or crystallization. The imidazole was present in the crystallization solution (0.2 M) and has been able to access the active site of the "closed" structure.

(2) The combination of tryptophan and imidazole causes the structural changes. The tryptophan has been bound in TPH in an open structure. Upon addition of imidazole, the closed structure forms. As shown in Figure 8, the imidazole and a water molecule satisfy four of the hydrogen bonds seen in the human cTPH1-Fe(III)·BH_2 structure, and it may be that this is enough to mimic the binding of BH_2 or BH_4 to TPH.

As mentioned above, BH_4 is believed to be the first substrate to bind in the aromatic amino acid hydroxylases. If this is the case and tryptophan accidently binds as the first substrate and the scenario where tryptophan alone is responsible for the structural change is true, the binding of BH_4 will be more difficult because the structure is closed. The closed TPH-Fe(III)·Trp structure would then be a nonproductive complex which gives a structural explanation for the observed tryptophan substrate inhibition (*18, 20, 36*) with a $K_{i,tryptophan}$ of 163 ± 24 μM for chicken cTPH1 (*20*). Substrate inhibition is also observed for TH, and Fitzpatrick has proposed the equivalent TH·Tyr forms a dead-end complex (*35*). Enzyme kinetics studies will be undertaken to determine the substrate binding order of TPH and the influence of imidazole on the enzyme kinetics. Additionally, crystallization without the imidazole will be used to attempt to clarify whether the imidazole has an effect on the structure.

Coordination of the Iron. The iron is coordinated by His273, His278, and Glu318. The coordination is shown in Figure 8A, and the bond lengths in chicken cTPH1-Fe(III)·Trp and human cTPH1-Fe(III)·BH_2 are summarized in Table 2 (and bond angles in Table S1 of the Supporting Information). The coordination by Glu318 is partially bidentate with bond lengths of 2.1 and 2.7 Å. Furthermore, an imidazole is coordinated to the iron with a bond length of 1.9 Å. The iron coordination is best described as a distorted trigonal bipyramidal coordination. No water molecules are coordinated to iron. The coordination of the iron in chicken cTPH1-Fe(III)·Trp is quite different from the octahedral iron coordination seen in the human cTPH1-Fe(III)·BH_2 structure (*18*) (see Figure 8B).

Table 2: Coordination Distances for Iron in Chicken cTPH1 Compared to Human cTPH1 (*18*) (chicken TPH1 residue numbering used)

	distance (Å)	
	chicken cTPH1-Fe(III)·Trp	human cTPH1-Fe(III)·BH_2
His273 N−Fe	2.1	2.1
His278 N−Fe	2.0	2.0
Glu318 Oε1−Fe	2.7	3.4
Glu318 Oε2−Fe	2.1	2.4
imidazole−Fe	1.9	−
water600−Fe	−	2.2
water601−Fe	−	2.2
water602−Fe	−	2.1

The iron in chicken cTPH1 is coordinated by the common 2-histidine-1-carboxylate facial triad motif seen in many dioxygen activating non-heme iron enzymes (*11*). The resting state in these enzymes has one face of the octahedral iron center coordinated by two histidines and one carboxylate and three water molecules on the opposite face. Such a resting state is seen for the octahedral iron center of human cTPH1-Fe(III)·BH_2 (Figure 8B). When substrate binds, one or two water molecules are usually released, leading to a more open five-coordinate iron site with an open site for O_2 (*11*). No water molecules are coordinated to the iron in chicken cTPH1, but instead, one imidazole is coordinated and the glutamate has a partial bidentate coordination. This five-coordinate iron therefore has an open site for O_2. A similar open iron coordination is seen in PAH-Fe(II)·BH_4·THA (PDB entry 1MMK), where the iron is coordinated by only the three coordinating residues, but with some electron density present close to the iron which could be a water molecule with low occupancy (*15*). In the PAH-Fe(II)·BH_4·NLE structure (PDB entry 1MMT) where THA is replaced with NLE, one water molecule is coordinated to the iron and still has an open site for O_2 (*15*). It is likely that the overall structural changes that occur upon substrate analogue binding reduce the affinity of the iron for water, thus yielding an open coordination site. The oxidation state of the iron may also influence the iron coordination. The

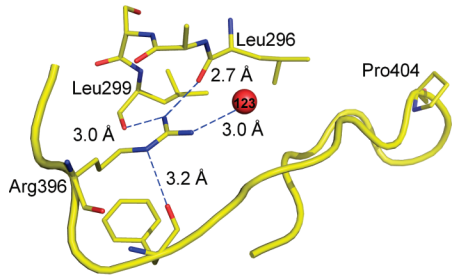

FIGURE 9: Interactions of Arg396 and the position of Pro404. Arg396 makes hydrogen bonds to Leu296, Leu299, Phe398, and water123 (shown as a red sphere). Pro404 functions as a turn residue in the C-terminal β-sheet.

iron is presumed to be in the ferric form, since the gel filtration and crystallization have been conducted in an aerobic atmosphere, and aerobic isolation of TH and PAH has resulted in the ferric form of the enzymes (*37, 38*). However, we have not made attempts to determine the oxidation state of the iron before or after the X-ray data collection.

Residues Arg396 and Pro404. The mutation corresponding to the R441H variant in human TPH2 is believed to be correlated with depression (*39*). Arg441 in human TPH2 corresponds to Arg396 in chicken TPH1. The Arg396 side chain makes hydrogen bonds to Leu296 O (2.7 Å), Leu299 O (3.0 Å), and Phe398 O (3.2 Å) (see Figure 9), and these hydrogen bonds are believed to be important in tying the C-terminal β-sheet to the rest of the catalytic domain (*40*). A mutation that changes Pro449 to arginine in human TPH2 (corresponds to Pro404 in chicken TPH1) has also been identified (*4*) and is believed to be important for the stability and catalytic activity of TPH (*39, 41, 42*). Structures of the catalytic and tetramerization domains of TH and PAH show that the C-terminal β-sheet is the link between the catalytic domain and the α-helix responsible for the tetramerization (*29, 40*). Pro404 in chicken TPH1 may have an important role in the formation of the turn of the C-terminal β-sheet, and mutations of this residue might lead to increased flexibility in the β-sheet formation, which destabilizes the tetramer.

CONCLUSION

In summary, the crystal structure of chicken cTPH1 has been determined to 1.9 Å resolution. The tryptophan substrate is bound close to the iron in a binding pocket distinct from the BH_4 binding pocket. The hydrophobic part of the tryptophan binding pocket is lined by residues Tyr236, Thr266, Pro269, His273, Phe314, Phe319, and Ile367, while the polar interactions of the tryptophan are with Thr266, Ile367, and Ser337 and a salt bridge to Arg258. The overall structure is more compact with two loops closing around the active site, when compared to the structure of human cTPH1.

ACKNOWLEDGMENT

We thank Flemming Hansen from the Department of Chemistry, University of Copenhagen, for collecting the data. We acknowledge the European Synchrotron Radiation Facility for provision of beam time and financial support from The Danish National Research Council (via Dansync).

SUPPORTING INFORMATION AVAILABLE

Sequence alignment of the catalytic domains of chicken TPH1 (with secondary structural elements), human TPH1, human TPH2, human PAH, and human TH, with the assigned secondary structural elements of the chicken cTPH1 structure, and a table with the bond angles of the iron coordination in the chicken and human cTPH1 structures. This material is available free of charge via the Internet at http://pubs.acs.org.

REFERENCES

1. Lovenberg, W., Jequier, E., and Sjoerdsma, A. (1967) Tryptophan hydroxylation: Measurement in pineal gland, brainstem and carcinoid tumor. *Science 155*, 217–219.
2. Lucki, I. (1998) The spectrum of behaviors influenced by serotonin. *Biol. Psychiatry 44*, 151–162.
3. Walther, D. J., Peter, J.-U., Bashammakh, S., Hörtnagl, H., Voits, M., Fink, H., and Bader, M. (2003) Synthesis of serotonin by a second tryptophan hydroxylase isoform. *Science 299*, 76.
4. Zhang, X., Beaulieu, J., Sotnikova, T. D., Gainetdinov, R. R., and Caron, M. G. (2004) Tryptophan hydroxylase-2 controls brain serotonin synthesis. *Science 305*, 217.
5. Walther, D. J., and Bader, M. (2003) A unique central tryptophan hydroxylase isoform. *Biochem. Pharmacol. 66*, 1673–1680.
6. Patel, P. D., Pontrello, C., and Burke, S. (2004) Robust and tissue-specific expression of TPH2 versus TPH1 in rat raphe and pineal gland. *Biol. Psychiatry 55*, 428–433.
7. Ganguly, S., Coon, S. L., and Klein, D. C. (2002) Control of melatonin synthesis in the mammalian pineal gland: The critical role of serotonin acetylation. *Cell Tissue Res. 309*, 127–137.
8. Fitzpatrick, P. F. (1999) Tetrahydropterin-dependent amino acid hydroxylases. *Annu. Rev. Biochem. 68*, 355–381.
9. Fitzpatrick, P. F. (2003) Mechanism of aromatic amino acid hydroxylation. *Biochemistry 42*, 14083–14091.
10. Pavon, J. A., and Fitzpatrick, P. F. (2006) Insights into the catalytic mechanisms of phenylalanine and tryptophan hydroxylase from kinetic isotope effects on aromatic hydroxylation. *Biochemistry 45*, 11030–11037.
11. Koehntop, K. D., and Emerson, J. P., Jr. (2005) The 2-His-1-carboxylate facial triad: A versatile platform for dioxygen activation by mononuclear non-heme iron(II) enzymes. *J. Biol. Inorg. Chem. 10*, 87–93.
12. Andersen, O. A., Flatmark, T., and Hough, E. (2001) High resolution crystal structures of the catalytic domain of human phenylalanine hydroxylase in its catalytically active Fe(II) form and binary complex with tetrahydrobiopterin. *J. Mol. Biol. 314*, 279–291.
13. Erlandsen, H., Fusetti, F., Martinez, A., Hough, E., Flatmark, T., and Stevens, R. C. (1997) Crystal structure of the catalytic domain of human phenylalanine hydroxylase reveals the structural basis for phenylketonuria. *Nat. Struct. Biol. 4*, 995–1000.
14. Andersen, O. A., Flatmark, T., and Hough, E. (2002) Crystal structure of the ternary complex of the catalytic domain of human phenylalanine hydroxylase with tetrahydrobiopterin and 3-(2-thienyl)-L-alanine, and its implications for the mechanism of catalysis and substrate activation. *J. Mol. Biol. 320*, 1095–1108.
15. Andersen, O. A., Stokka, A. J., Flatmark, T., and Hough, E. (2003) 2.0 Å resolution crystal structure of the ternary complex of human phenylalanine hydroxylase with tetrahydrobiopterin and 3-(2-thienyl)-L-alanine, or L-norleucine: Substrate specificity and molecular motions related to substrate binding. *J. Mol. Biol. 333*, 747–757.
16. Daubner, S. C., McGinnis, J. T., Gardner, M., Kroboth, S. L., Morris, A. R., and Fitzpatrick, P. F. (2006) A flexible loop in tyrosine hydroxylase controls coupling of amino acids hydroxylation to tetrahydropterin oxidation. *J. Mol. Biol. 359*, 299–307.
17. Sura, G. R., Lasagna, M., Gawandi, V., Reinhart, G. D., and Fitzpatrick, P. F. (2006) Effects of ligands on the mobility of an active-site loop in tyrosine hydroxylase as monitored by fluorescence anisotropy. *Biochemistry 45*, 9632–9638.
18. Wang, L., Erlandsen, H., Haavik, J., Knappskog, P. M., and Stevens, R. C. (2002) Three-dimensional structure of human tryptophan hydroxylase and its implications for the biosynthesis of the neurotransmitters serotonin and melatonin. *Biochemistry 41*, 12569–12574.

19. Erlandsen, H., Bjørgo, E., Flatmark, T., and Stevens, R. C. (2000) Crystal structures and site-specific mutagenesis of pterin-bound human phenylalanine hydroxylase. *Biochemistry 39*, 2208–2217.
20. Nielsen, M. S., Petersen, C. R., Munch, A., Vendelboe, T. V., Boesen, J., Harris, P., and Christensen, H. E. M. (2008) A simple two step procedure for purification of the catalytic domain of chicken tryptophan hydroxylase 1 in a form suitable for crystallization. *Protein Expression Purif. 57*, 116–126.
21. Kabsch, W. (1993) Automatic processing of rotation diffraction data from crystals of initially unknown symmetry and cell constants. *J. Appl. Crystallogr. 26*, 795–800.
22. Murshudov, G. N., Vagin, A. A., and Dodson, E. J. (1997) Refinement of macromolecular structures by the maximum-likelihood method. *Acta Crystallogr. D53*, 240–255.
23. Collaborative Computational Project, Number 4 (1994) The CCP4 suite: Programs for protein crystallography. *Acta Crystallogr. D50*, 760–763.
24. Emsley, P., and Cowtan, K. (2004) Coot: Model-building tools for molecular graphics. *Acta Crystallogr. D60*, 2126–2132.
25. Laskowski, R. A., MacArthur, M. W., Moss, D. S., and Thornton, J. M. (1993) PROCHECK: A program to check the stereochemical quality of protein structures. *J. Appl. Crystallogr. 26*, 283–291.
26. Lu, G. (2000) TOP: A new method for protein structure comparisons and similarity searches. *J. Appl. Crystallogr. 33*, 176–183.
27. DeLano, W. L. (2002) The PyMOL Molecular Graphics System, DeLano Scientific, Palo Alto, CA.
28. Hayward, S., and Berendsen, H. J. C. (1998) Systematic analysis of domain motions in proteins from conformational change: New results on citrate synthase and T4 lysozyme. *Proteins 30*, 144–154.
29. Goodwill, K. E., Sabatier, C., Marks, C., Raag, R., Fitzpatrick, P. F., and Stevens, R. C. (1997) Crystal structure of tyrosine hydroxylase at 2.3 Å and its implications for inherited neurodegenerative diseases. *Nat. Struct. Biol. 4*, 578–585.
30. Jiang, G. C.-T., Yohrling, G. J., Schmitt, I. V. J. D., and Vrana, K. E. (2000) Identification of substrate orienting and phosphorylation sites within tryptophan hydroxylases using homology-based molecular modeling. *J. Mol. Biol. 302*, 1005–1017.
31. McKinney, J., Teigen, K., Frøystein, N. Å., Salaün, C., Knappskog, P. M., Haavik, J., and Martínez, A. (2001) Conformation of the substrate and pterin cofactor bound to human tryptophan hydroxylase. Important role of Phe313 in substrate specificity. *Biochemistry 40*, 15591–15601.
32. Daubner, S. C., Moran, G. R., and Fitzpatrick, P. F. (2002) Role of tryptophan hydroxylase Phe313 in determining substrate specificity. *Biochem. Biophys. Res. Commun. 292*, 639–641.
33. Daubner, S. C., Melendez, J., and Fitzpatrick, P. F. (2000) Reversing the substrate specificities of phenylalanine and tyrosine hydroxylase: Aspartate 425 of tyrosine hydroxylase is essential for L-DOPA formation. *Biochemistry 39*, 9652–9661.
34. Volner, A., Zoidakis, J., and Abu-Omar, M. M. (2003) Order of substrate binding in bacterial phenyalanine hydroxylase and its mechanistic implication for pterin-dependent oxygenases. *J. Biol. Inorg. Chem. 8*, 121–128.
35. Fitzpatrick, P. F. (1991) Steady-state kinetic mechanism of rat tyrosine hydroxylase. *Biochemistry 30*, 3658–3662.
36. Moran, G. R., Daubner, S. C., and Fitzpatrick, P. F. (1998) Expression and characterization of the catalytic core of tryptophan hydroxylase. *J. Biol. Chem. 273*, 12259–12266.
37. Ramsey, A. J., Hillas, P., and Fitzpatrick, P. F. (1996) Characterization of the active site iron in tyrosine hydroxylase. *J. Biol. Chem. 271*, 24395–24400.
38. Fisher, D. B., Kirkwood, R., and Kaufman, S. (1972) Rat liver phenylalanine hydroxylase, an iron enzyme. *J. Biol. Chem. 247*, 5161–5167.
39. Zhang, X., Gainetdinov, R. R., Beaulieu, J. M., Sotnikova, T. D., Burch, L. H., Williams, R. B., Schwartz, D. A., Krishnan, K. R., and Caron, M. G. (2005) Loss-of-function mutation in tryptophan hydroxylase-2 identified in unipolar major depression. *Neuron 45*, 11–16.
40. Fusetti, F., Erlandsen, H., Flatmark, T., and Stevens, R. C. (1998) Structure of tetrameric human phenylalanine hydroxylase and its implications for phenylketonuria. *J. Biol. Chem. 273*, 16962–16967.
41. Sakowski, S. A., Geddes, T. J., and Kuhn, D. M. (2006) Mouse tryptophan hydroxylase isoform 2 and the role of proline 447 in enzyme function. *J. Neurochem. 96*, 758–765.
42. Winge, I., McKinney, J. A., Knappskog, P. M., and Haavik, J. (2007) Characterization of wild type and mutant forms of human tryptophan hydroxylase 2. *J. Neurochem. 100*, 1648–1657.

BI8015263